# Disentangling the Delayed Choice Quantum Eraser

Thomas V. Higgins

***Abstract***

This paper examines the experimental setup and physics behind the Delayed Choice Quantum Eraser, with an emphasis on the significance of the phase-matching condition within the nonlinear BBO crystal used to create the entangled photons. The paper takes the reader step-by-step through the experiment and the physics governing each element of it. A general undergraduate understanding of quantum mechanics is assumed.

*Published by tvhiggins.com March 27, 2025*

***Introduction***

Perhaps the most insightful proclamation ever made about quantum mechanics came from one of its most important contributors, Richard P. Feynman, who once declared, "Nobody understands quantum mechanics." Despite being the most successful theory about the physical universe ever conceived by humankind, nobody can truthfully claim that it makes total sense to them, because it just doesn't. Plus, the more we learn about quantum theory, and the more sophisticated our experiments become, the stranger it gets.

Such is the case with the now famous delayed choice quantum eraser experiment, which was first described by Kim and others in 2000. [1] Since then, many have attempted to interpret and explain its results, including me and my late colleague E. Brian Treacy in 2005. [2] Some interpretations are more lucid than others [3] [4] [5], but in most cases the experiment seems to engender more confusion than clarity, especially in articles written for the general audience. Chief among these misinterpretations is the notion that the experiment proves that the present can affect the past—so-called "retrocausality." Color me doubtful about this one. If the present could affect the past, there are a few things I'd like to undo. But I personally don't think it's possible. Who knows, though, maybe one day someone will prove me wrong about that, too. Nobody really understands quantum mechanics. Nevertheless, this paper offers yet another attempt to explain what might be going on in the delayed choice quantum eraser.

***Young's double-slit with a pivotal quantum twist***

Figure 1 shows the basic setup of the original experiment. At the bottom of the figure, UV light (351.1-nm) from an argon-ion laser (blue arrows) irradiates a double-slit, just like in Young's classic experiment. However, the similarity to Young's experiment quickly vanishes next, because the wavefunction of each coherent UV photon that passes through the two slits is promptly used to pump two regions (1 and 2 in Figure 1) of a β-Barium Borate (BBO) crystal. Understanding what happens next within this nonlinear crystal is the key to understanding how the experiment works, because that's where much of the quantum magic happens.

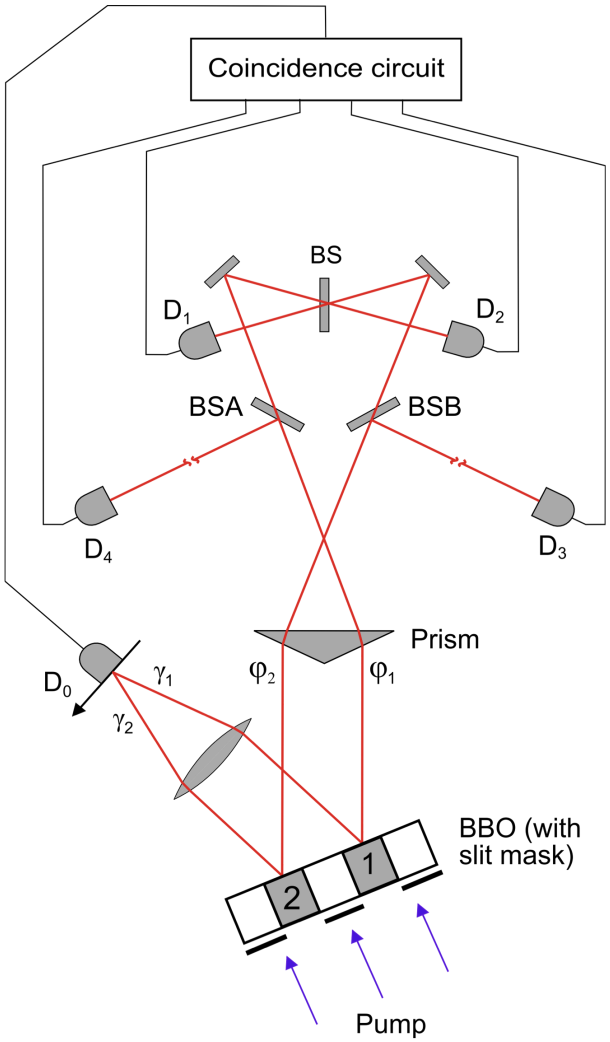


Figure 1

Most of the pumping photons just pass right through the BBO crystal. Type-II spontaneous parametric down conversion, or SPDC for short, is a very inefficient process. But each pump photon of a lucky few (1 in $10^6$) will be transformed within the crystal into two new photons having twice the wavelength (702.2 nm) and therefore half the frequency or energy.

Now, there are a few important details to recognize about SPDC. First, down conversion is a non-local quantum process, meaning that both regions of the crystal participate in the creation of each photon pair from each pump photon. Consequently, you can't know which region a down-converted photon pair came from: region 1, region 2, or both. In this regard, the quantum physics mimics the classic double-slit experiment.

Second, unlike the double-slit experiment, the BBO crystal has a thickness within which SPDC takes place. Kim et al. used a 0.3-mm-thick crystal in their original experiment. This would ordinarily scramble the phases of wavefronts emerging from the crystal if it weren't for another very important condition: phase matching.

In my opinion, the phase-matching condition is the most important SPDC property in this experiment next to entanglement, because the quantum eraser wouldn't work without it, which I will get to soon. Even so, most explanations of this experiment that I've read fail to even mention the phase matching condition, oddly enough.

The phase-matching condition follows naturally from the conservation laws, whereby the sum of the energy (or the momentum) of the two down-converted photons (signal γ and idler φ in Figure 1) must equal the energy (or momentum) of the pump photon. Mathematically this is expressed as:

$$\mathbf{k}_p = \mathbf{k}_s + \mathbf{k}_i \qquad \text{Eq. 1}$$

$$\omega_p = \omega_s + \omega_i\,, \qquad \text{Eq. 2}$$

where $\mathbf{k}_p$, $\mathbf{k}_s$, and $\mathbf{k}_i$ represent the wavevectors of the pump, signal, and idler photons, respectively, and $\omega_p$, $\omega_s$, and $\omega_i$ represent their respective angular frequencies. The wavevectors $\mathbf{k}_\alpha$ ($\alpha$ = p, s, i) directly express the photons' momenta through the de Broglie relation $\mathbf{p}_\alpha = h\mathbf{k}_\alpha/2\pi$, and $\omega_\alpha$ relates to the photons' energies through Planck's relation $E_\alpha = h\omega_\alpha/2\pi$ (h = Planck's constant). The phase velocities ($\mathbf{v}_\alpha$) of pump, signal, and idler also are linked by $\mathbf{v}_\alpha = \omega_\alpha/\mathbf{k}_\alpha$, which lets us to rewrite Eq. 1 as $\omega_p/\mathbf{v}_p = \omega_s/\mathbf{v}_s + \omega_i/\mathbf{v}_i$. Therefore, phase velocities must match the pump, too.

These factors and others—such as refractive indexes along the birefringent crystal axes, polarizations, and temperature—govern the phase matching condition. But the bottom line is that signal and idler must stay in-phase with the pump laser's coherent wavefront as they propagate through the crystal. There are basically two ways in which this can happen: either their phase sum equals the pump's phase or their sum is π radians out of phase. With any other phase sum, the SPDC efficiency suffers greatly. These two complementary phase-matching conditions are called "symmetric" and "antisymmetric," respectively. Phase-matching therefore couples the idler and signal phases to the pump's coherent wavefront symmetrically and antisymmetrically.

Finally, there are three other important Type-II SPDC attributes to mention: 1) the pump photon creates the signal/idler pair simultaneously, 2) signal and idler polarization states are mutually orthogonal, and 3) the signal/idler wavefunction is entangled. This entangled-pair state is quantum mechanically described in Dirac notation as: $1/\sqrt{2}\ (|\Psi_{\gamma H}\rangle|\Psi_{\varphi V}\rangle + |\Psi_{\gamma V}\rangle|\Psi_{\varphi H}\rangle)$, where $|\Psi_{\gamma H}\rangle|\Psi_{\varphi V}\rangle$ denotes a tensor product $\Psi_{\gamma H} \otimes \Psi_{\varphi V}$, and subscripts $\gamma_H$, $\varphi_V$ and $\gamma_V$, $\varphi_H$ denote horizontally and vertically polarized signal/idler pairs from the BBO. Entanglement basically links two wavefunctions together as one across space and time. Therefore, what you do to one

immediately affects what you know about the other, no matter how far apart they may get. They are correlated throughout spacetime. Einstein, who was famously bothered by quantum entanglement, called it "spooky action at a distance." And it is just that—spooky.

**The remaining experimental setup**

Let's dissect what's going on in the rest of the delayed choice quantum eraser setup. Signal photons (γ) emitted from the two BBO regions are directed off to the left in Figure 1, where they encounter a lens that focuses them onto the scanning detector $D_0$. This detector looks for any interference fringes that might appear along the focal plane where the two beams intersect.

Idler photons (φ) exit the BBO to a separate area of the setup in Figure 1, where they encounter a prism, three beamsplitters (BSA, BSB, BS), two mirrors, and four detectors ($D_1$, $D_2$, $D_3$, $D_4$). Optical path lengths from the BBO to these four detectors $D_\varphi$ (φ=1-4) are all made equal, but they also are intentionally made longer than the optical path length from the BBO to $D_0$. This creates a time delay between the detections of each idler photon and its entangled signal-photon twin. In the original experiment, this delay amounts to "at least 8 ns."

Each of the $D_\varphi$ detectors is also electronically linked with $D_0$ for coincidence detection (see Figure 1 again). Since each signal/idler pair is created simultaneously, coincidence detections will generate a ledger containing four subsets of synchronized event data. Each detection event at $D_0$ will therefore have a corresponding detection of its entangled twin 8 ns later at one of the $D_\varphi$ detectors.

**The experiment in action**

Let's now look at what happens when we fire up the laser and start taking data. The first thing to notice on the signal-photon side is that we don't see any interference fringes at $D_0$ (see Figure 2b). Those who know how the double-slit experiment works would expect to see fringes (see Figure 2a), so this may come as a surprise. Let's examine what might be happening here.

One quantum mechanical explanation for the absence of an interference pattern at $D_0$ is that the wavefunction of each signal-photon at $D_0$ is in a superposition of four complementary

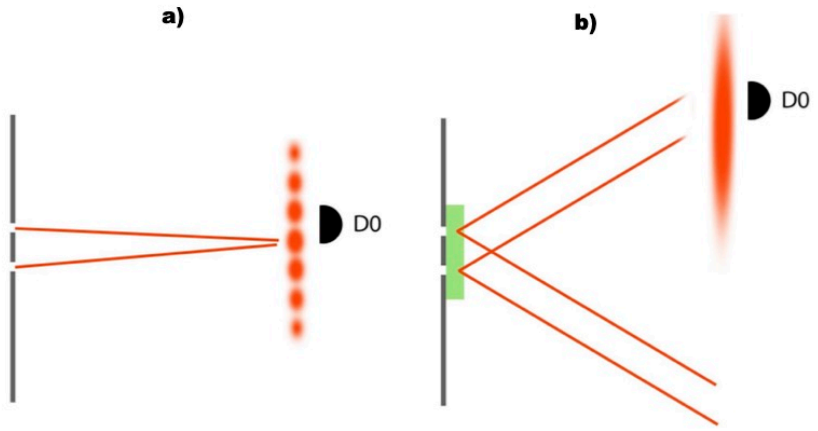


Figure 2 (from [3])

SPDC states: region 1 acting alone, region 2 acting alone, regions 1 and 2 acting together in-phase (symmetric), and regions 1 and 2 acting together antiphase (antisymmetric).

Another quantum mechanical explanation is that entanglement destroys interference. The reason given for this interpretation is that the entangled photons act as tags to one another. This creates the potential to determine which-path information, and even the potential for having such information destroys interference.

If entanglement destroys interference, the idler side of the experiment is designed to recover the four SPDC quantum states virtually by using the coincidence-detection data. Here's how that works (refer to Figure 1, again). Idler photons emitted from the BBO first encounter the 50/50 beamsplitters BSA and BSB, where there's a 50/50 chance $\varphi_2$ will get diverted to $D_3$ and a 50/50 chance $\varphi_1$ will go to $D_4$. The purpose here is to glean which-path information.

Idler photons that don't get deflected to $D_3$ or $D_4$ proceed via the two mirrors to beamsplitter BS. The motive of BS is to "erase" which-path information by making it impossible to know which BBO region the idler photon came from. This part of the experiment is called—you guessed it—the "quantum eraser."

The joint wavefunction due to the quantum eraser can be modeled mathematically as,

$$\Psi = 1/\sqrt{2}\,[\Psi_{D1} \otimes (-\Psi\gamma_1 - \Psi\gamma_2)] + 1/\sqrt{2}\,[\Psi_{D2} \otimes (\Psi\gamma_1 - \Psi\gamma_2)], \qquad \text{Eq. 3} \quad [5]$$

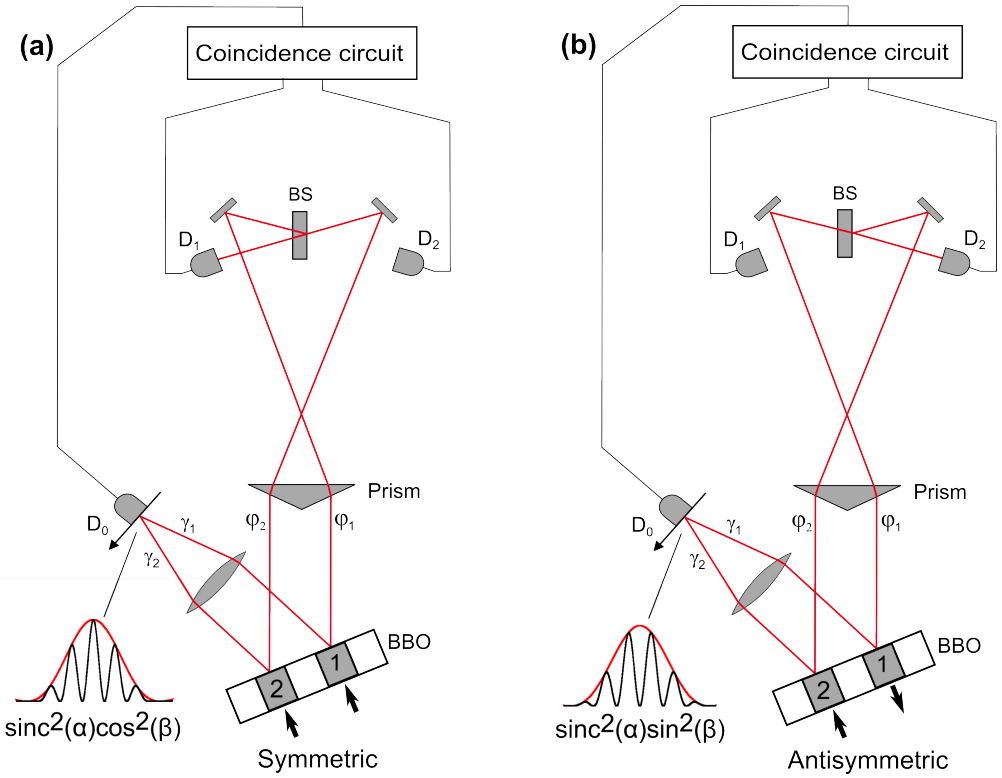


Figure 3

which links idler (φ) detections at $D_1$, $D_2$ to the signal's (γ) phase states, and where the +/- signs within the brackets account for the π-radian phase shifts encountered by the idler wavefunction at both the mirrors and the beamsplitter BS. The phase shift at the mirrors is always π radians. The phase shift at beamsplitter BS, however, depends crucially on which direction the wavefunction is coming from and whether it is reflected or transmitted at BS. If, for example, we consider idler $\varphi_2$, there is a 50% probability that it will either be reflected to $D_2$ or transmitted to $D_1$ (see Figure 3). If it gets reflected from BS to $D_2$, then it experiences a π-radian phase shift. But, if it's transmitted to $D_1$, it undergoes no phase shift. On the other hand, if we're talking about $\varphi_1$, an internal reflection that occurs within the glass substrate of BS, which redirects it to $D_1$, experiences no phase shift, and neither does a transmission of $\varphi_1$ through BS to $D_2$.

Beamsplitter BS therefore has a very useful sorting capacity. Idler wavefunctions in a superposition of symmetric/antisymmetric phase states are sorted by BS into two separate sets. $D_2$ clicks for antisymmetric states, and $D_1$ clicks for symmetric ones. This comes about from the

asymmetric, collinear overlap (interference) of the symmetric and antisymmetric phase states at the Mach-Zehnder-style interferometer that defines the quantum eraser. For symmetric phases, the idler photon's wavefunction interferes constructively with itself in the direction of $D_1$ and destructively toward $D_2$. For antisymmetric phases, the wavefunction interferes destructively in the direction of $D_1$ and constructively toward $D_2$. Consequently, the path from BS to $D_2$ is dark for symmetric states while the path from BS to $D_1$ is dark for antisymmetric ones (see Figure 3).

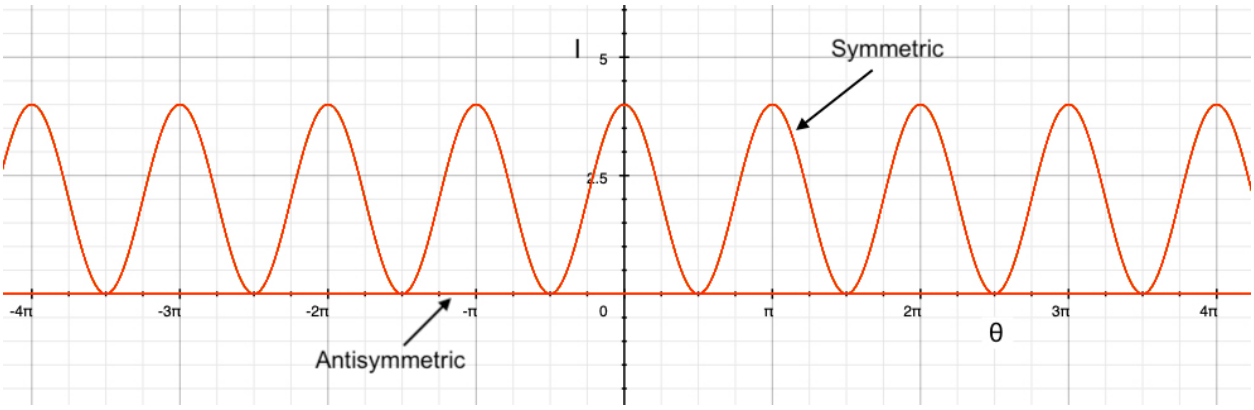


Figure 4

Figure 4 models the collinear interference of the symmetric/antisymmetric idler wavefunctions that exit the BBO, as seen at detector $D_1$. The red plots simulate intensity and phase conditions of the detected photons emitted by the two BBO regions using the equation:

$$I = [\cos(\theta_1 + n\pi) + \cos(\theta_2 + m\pi)]^2 , \qquad \text{Eq. 4}$$

where n=0-10 and m=0-10. The ordinate of the graph represents intensity, the abscissa tracks the phase, and θ is the initial phase of each region, which is made equal to the coherent pump laser through phase matching. For symmetric phases, m and n are either both even or both odd integers, which symbolize whole-wavelength phase shifts between BBO regions 1 and 2. For antisymmetric phases, either m is even and n is odd or m is odd and n is even, which symbolize half-wavelength phase shifts between the two BBO regions. (I used ten integers of the multiples m and n as a way to help visualize several phase-matched waves over a distance of five wavelengths, which is about 3.5 microns or >1% of the BBO thickness.)

Note in Figure 4 that symmetric phases interfere constructively with high intensity while destructive antisymmetric interference yields zero intensity at $D_1$. However, the opposite is true at $D_2$, where the antisymmetric phase interferes constructively. But this happens only because of the asymmetric phase shift at BS, which converts an antisymmetric phase from the BBO into a symmetric one, which then interferes constructively at $D_2$.

**Analysis, questions, and discussion**

Now we can paint a fuller picture of how the delayed choice quantum eraser works. $D_0$-$D_1$ coincidence detections flag the symmetric state, $D_0$-$D_2$ coincidences flag the antisymmetric state, and $D_0$-$D_3$ or $D_0$-$D_4$ coincidences yield which-path information. So, the delayed choice quantum eraser is actually a sorting machine. It uses coincidence detections that exploit the tagging feature of entanglement, along with the sorting feature of the quantum eraser, in order to parse the symmetry and which-path information of the signal photons.

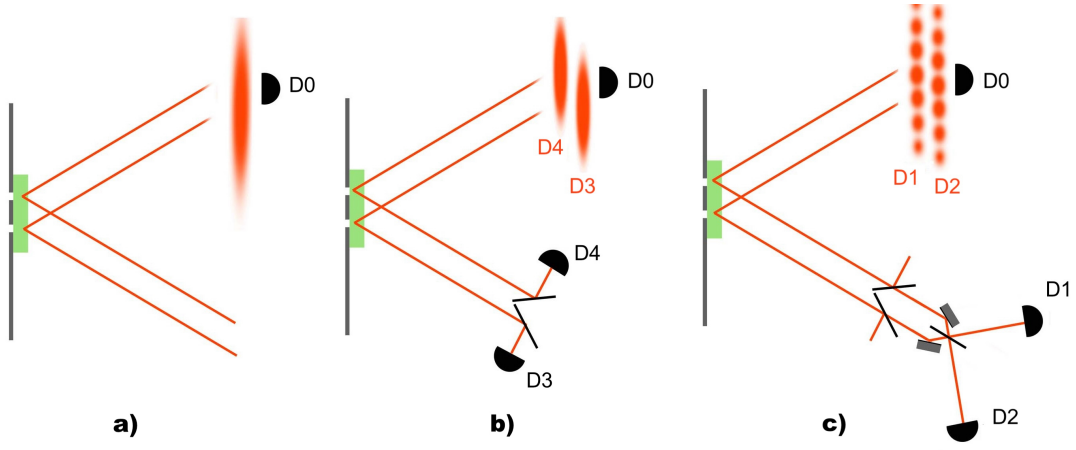


Figure 5 (from [3])

What looks like a complete lack of interference at $D_0$ in Figure 5a actually hides a superposition of four complementary signal-photon states: $\Psi\gamma_1$, $\Psi\gamma_2$, $(\Psi\gamma_1 + \Psi\gamma_2)$, and $(\Psi\gamma_1 - \Psi\gamma_2)$. Figures 5b and 5c visualize the photon distributions of each state separately. Note that when you add together the two states of Figure 5b or 5c, you get the distribution shown in Figure 5a. The complementary superposition shown in Figure 5c is also depicted by the curves

drawn in Figure 3. Those curves show how the $D_0$-$D_1$ and $D_0$-$D_2$ interference distributions of $sinc^2cos^2$ and $sinc^2sin^2$ (black) add up to a $sinc^2$ distribution (red), as observed in the original experiment.

So, in some sense, both reasons given earlier for the lack of interference patterns at $D_0$ seem justified. But in order to "see" the complementary interference patterns of Figure 5c, for example, we need to plot out the coincidence data collected by $D_0$-$D_1$ and $D_0$-$D_2$. Eq. 3 describes the joint wavefunction at work here. When $D_1$ clicks, the wavefunction of Eq. 3 collapses to $(-\Psi\gamma_1 - \Psi\gamma_2)$. Ignoring normalization factors, we can calculate the modulus squared as $(-\Psi\gamma_1 - \Psi\gamma_2)(-\Psi\gamma_1 - \Psi\gamma_2)^*$, where $(-\Psi\gamma_1 - \Psi\gamma_2)^*$ defines the complex conjugate. The result is,

$$|\Psi|^2 = |\Psi\gamma_1|^2 + |\Psi\gamma_2|^2 + 2|\Psi\gamma_2||\Psi\gamma_1|. \qquad \text{Eq. 5}$$

Substituting ordinary plane waves $A_1e^{i\varphi 1}$ for $\Psi\gamma_1$ and $A_2e^{i\varphi 2}$ for $\Psi\gamma_2$ above, where $A_1$, $A_2$ are the wave amplitudes and $\varphi_1, \varphi_2$ are their phases, we get $(-A_1e^{i\varphi 1} - A_2e^{i\varphi 2})(-A_1e^{-i\varphi 1} - A_2e^{-i\varphi 2})$, yielding the intensity distribution of,

$$I = A_1^2 + A_2^2 + 2A_1A_2\cos(\varphi_2 - \varphi_1), \qquad \text{Eq. 6}$$

which describes the classic interference pattern of a double slit irradiated by a plane wave.

For the antisymmetric wavefunction, Eq. 3 collapses to $(\Psi\gamma_1 - \Psi\gamma_2)$ each time $D_2$ clicks. Using the same plane-wave substitutions as above, the intensity distribution looks like,

$$I = A_1^2 + A_2^2 - 2A_1A_2\cos(\varphi_2 - \varphi_1). \qquad \text{Eq. 7}$$

Eq. 7 describes a double-slit pattern complementary to the one portrayed in Eq. 6. Together, Eqs. 6 and 7 mimic the patterns we see in Figure 5c. Both of these equations are didactic representations, though. Again, the interference patterns in the original experiment are a little different because of the diffraction from finite slit-widths, etc., as we saw earlier in Fig. 3 with the $sinc^2cos^2$ and $sinc^2sin^2$ plots. Nevertheless, the fundamental physics is the same.

To "see" the complementary patterns of Figure 5b, we need to plot out the coincidence data of $D_0$-$D_3$ and $D_0$-$D_4$. Entangled superpositions of the orthogonally polarized photon pairs created in both regions of the BBO can be generally described in Dirac notation as

$$|\Psi> = 1/\sqrt{2}\ [(|\Psi_{\gamma 1H}>|\Psi_{\varphi 1V}> + |\Psi_{\gamma 1V}>|\Psi_{\varphi 1H}>) + (|\Psi_{\gamma 2H}>|\Psi_{\varphi 2V}> + |\Psi_{\gamma 2V}>|\Psi_{\varphi 2H}>)], \qquad \text{Eq. 8}$$

where the H and V subscripts symbolize horizontal and vertical polarization states, respectively. Eq. 8 includes both variants of the polarization states that can exist for multiple pairs of photons created in both BBO regions. For a single photon pair, this equation reduces to either

$$|\Psi> = 1/\sqrt{2}\ (|\Psi_{\gamma 1H}>|\Psi_{\varphi 1V}> + |\Psi_{\gamma 2H}>|\Psi_{\varphi 2V}>) \text{ or} \qquad \text{Eq. 9}$$

$$|\Psi> = 1/\sqrt{2}\ (|\Psi_{\gamma 1V}>|\Psi_{\varphi 1H}> + |\Psi_{\gamma 2V}>|\Psi_{\varphi 2H}>), \qquad \text{Eq. 10}$$

for the alternative orthogonal polarizations. Since the signal and idler wavefunctions are orthogonal, the modulus squared of Eq. 9 becomes

$$|\Psi|^2 = 1/2\ (|\Psi_{\gamma 1H}|^2\ |\Psi_{\varphi 1V}|^2 + |\Psi_{\gamma 2H}|^2\ |\Psi_{\varphi 2V}|^2), \qquad \text{Eq. 11} \quad [5]$$

and the interference term that we saw in Eq. 5 vanishes. Thus, the entangled state of Eq. 9 collapses to $1/\sqrt{2}\ |\Psi_{\gamma 1H}>|\Psi_{\varphi 1V}>$ if $D_4$ clicks, yielding a modulus squared of $1/2\ |\Psi_{\gamma 1H}|^2\ |\Psi_{\varphi 1V}|^2$. If $D_3$ clicks, it collapses to $1/\sqrt{2}\ |\Psi_{\gamma 2H}>|\Psi_{\varphi 2V}>$ with a modulus squared of $1/2\ |\Psi_{\gamma 2H}|^2\ |\Psi_{\varphi 2V}|^2$. Since $D_0$ is scanning only the signal-photon's ($\gamma$) spatial distribution, $D_0$-$D_4$ data therefore uncovers the clump pattern of $|\Psi_{\gamma 1H}|^2$, and $D_0$-$D_3$ data reveals the clump pattern of $|\Psi_{\gamma 2H}|^2$ (see Figure 5b). Eq. 10 will collapse in a similar way for the alternative polarization states.

Notably, it doesn't matter whether $D_0$ clicks first or $D_\varphi$ does. From the perspective of wavefunction collapse, it's just as valid to interpret a signal-photon detection collapsing the idler wavefunction as it is the other way around. The correlations between entangled states exist across spacetime. A measurement made on one entangled quantum, and its resulting wavefunction collapse, does not determine the state of the other; rather, it reveals a correlation

between the two that's independent of time and space, for as long as they remain entangled. What matters is which correlation you choose to reveal, not when you choose to do it. So much for spooky "retrocausality."

It is also widely argued that entanglement kills or reduces interference, which is called decoherence. Here's just one example: "As soon as the signal photon gets entangled [with the idler], the photon states lose their coherence." [5] Yet, in this experiment, interference is still alive and well among entangled idler photons at the quantum eraser. Some level of coherence must exist for it to function, despite entanglement. It is the coherent phase-matching condition within the BBO that makes possible the collinear sorting done by the interferometer at the eraser. You can't have a working interferometer without coherent interference. It's literally in the name. Therefore, if coherent idler photons can interfere, so should coherent signal photons. Both are phase-matched by the same BBO, as described earlier.

One very pertinent question to ask, then, would be this: Can the superposed, complementary signal-photon states somehow be physically (optically) separated, too? The experiment separates these states virtually using coincidence detection and the quantum property of entanglement, but if there also were a way to optically sort at least the symmetric/ antisymmetric states—as is done with idler wavefunctions at the quantum eraser—would we actually see the fringes of Figure 5c? I personally don't see how to do this, but if it's only possible to disentangle entangled states virtually, what does this tell us about non-locality, spacetime, entanglement, and wavefunctions in general? Wavefunction entanglement does seem to transcend the dimensions of time and space. That's what makes this experiment, and others like it, so fascinating to me. Feynman would be smiling.